

Characteristics of Proton CT Images Reconstructed with Filtered Backprojection and Iterative Projection Algorithms

Scott N. Penfold, *Student Member, IEEE*, Reinhard W. Schulte, Yair Censor, Vladimir Bashkurov, and Anatoly B. Rosenfeld, *Member, IEEE*

Abstract– In early studies of proton computed tomography (pCT), images were reconstructed with the fast and robust filtered backprojection (FBP) algorithm. Due to multiple Coulomb scattering of the protons within the object, the straight line path assumption of FBP resulted in poor spatial resolution. In an attempt to improve spatial resolution, a formalism to predict the proton path of maximum likelihood through the image space was created. The use of these paths with the iterative algebraic reconstruction technique (ART), have shown an improvement in spatial resolution, but also an increase in image noise, resulting in poor density resolution.

In this work, we propose a reconstruction method that attempts to optimize both spatial and density resolution of pCT images. The new reconstruction approach makes use of the block-iterative diagonally relaxed orthogonal projections (DROP) algorithm with an initial FBP-reconstructed image estimate. Reconstruction of Monte Carlo simulated pCT data sets of spatial and density resolution phantoms demonstrated that the combined reconstruction approach resulted in better spatial resolution than the FBP algorithm alone and better density resolution than the DROP algorithm starting from a uniform initial image estimate.

I. INTRODUCTION

Proton computed tomography (pCT) was first experimentally investigated as an alternative to diagnostic X-ray CT in the 1970s and early 1980s [1,2]. Although dose advantages were found with pCT, greater development efforts were made with X-ray CT due to the greater spatial resolution achievable and the lack of proton accelerators. With the expansion of proton therapy over the last decade, interest has again been placed in pCT. Now, pCT is being developed as a means for maximizing the potential benefits of proton therapy.

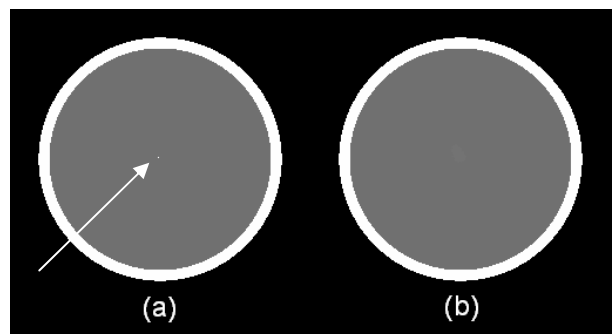
The pCT design proposed by Schulte *et al.* [3] employs position sensitive silicon tracking planes at the boundaries of the image space, to allow for individual proton entry and exit position and direction measurements. Proton exit energy is also measured with downstream scintillation crystal

calorimeters. The energy lost by individual protons is converted to an integral relative stopping power (RSP) by the Bethe-Bloch relationship. This forms the basis for a reconstruction of the RSP map.

In a number of previous pCT reconstruction studies [1,2,4], the geometrical path of protons through the image space was assumed to be a straight line. This assumption allowed the use of the fast and robust filtered backprojection (FBP) reconstruction algorithm. These studies found that pCT images reconstructed with FBP exhibited good density contrast (low noise) in comparison to X-ray CT, but poor spatial resolution. The poor spatial resolution is due to multiple Coulomb scattering (MCS) within the object, making the straight line approximation inaccurate.

Li *et al.* [5] showed that superior spatial resolution can be achieved when a path of maximum likelihood [6,7] that takes MCS into account is used instead of the straight-line assumption. The algebraic reconstruction technique (ART) [8], an iterative projection method for solving a system of equations, has been found to deal well with these nonlinear paths. However, accounting for MCS in the reconstruction is a computer intensive procedure, so we are looking to inherently parallel block-iterative or string-averaging iterative projection methods executed on multiple processors simultaneously as the next step forward.

In this study, we investigated a reconstruction method that combines FBP with an iterative projection algorithm in the reconstruction of simulated pCT data sets. The new reconstruction approach uses the block-iterative diagonally relaxed orthogonal projection (DROP) algorithm [9] with an FBP-reconstructed image as the initial image estimate. Thus, the FBP initial estimate provides a low-noise starting point for the iterative procedure.



Manuscript received November 13, 2009.

This work was supported in part by the Cancer Institute NSW, Australia under Grant No. 08/RSA/1-02.

S. N. Penfold and A. B. Rosenfeld are with the Centre for Medical Radiation Physics, University of Wollongong, Wollongong, NSW 2522 Australia (e-mail: snp75@uow.edu.au).

R. W. Schulte and V. Bashkurov are with the Department of Radiation Medicine, Loma Linda University Medical Center, Loma Linda, CA 92354 USA.

Y. Censor is with the Department of Mathematics, University of Haifa, Mt. Carmel, Haifa, 31905 Israel.

Fig. 1. Cross-sections of the cylindrical phantoms used in the GEANT4 pCT simulations. (a) Phantom with central dense structure (indicated by arrow) to quantify spatial resolution. (b) Phantom with uniform interior.

II. METHODS

A. Proton CT Simulation

The Monte Carlo software toolkit GEANT4 [10] was used to simulate a realistic pCT system. A monoenergetic 200 MeV proton beam was generated in a vacuum environment simulating the proton accelerator. The beam exited vacuum through a 25 μm thick titanium foil and was subsequently collimated with a 7 cm long, 2 mm hole brass collimator. A 2.5 mm thick lead scattering foil was placed on the downstream face of the brass collimator to generate a proton cone beam.

A cylindrical phantom was placed 2 m downstream of the lead scattering foil. Cross sections of the cylindrical phantoms used for spatial and density resolution studies are shown in Fig. 1(a) and 1(b), respectively. Both phantoms had a diameter of 16 cm containing materials of brain and cranial bone chemical composition and density as set out by the International Commission on Radiological Protection (ICRP) [11]. The spatial resolution phantom also contained a central rectangular prism structure, having a cross-section of $(0.82 \times 0.82) \text{ mm}^2$, equal to the reconstruction pixel size. The density of this structure was 20 times greater than the surrounding material.

Four 2D position sensitive silicon modules were centered at -30 cm, -20 cm, 20 cm and 30 cm relative to the phantom. Each module consisted of one x and one y dimensionally sensitive 30×5 cm silicon strip detector 400 μm thick. The resolution of individual silicon strip detectors was set at 228 μm . Note that thickness and resolution match the specifications of a prototype pCT scanner currently constructed at the University of California at Santa Cruz,

A single cesium iodide crystal calorimeter was placed downstream of the exiting tracking modules. The crystal shape corresponded to a segment of a spherical shell, mimicking the *segmented* crystal geometry currently under development for the prototype pCT system.

180 projection angles in 2 degree intervals were simulated for each phantom. In each projection angle, the position in each tracking plane and energy deposited in the calorimeter was recorded for 200,000 protons.

B. Proton CT Filtered Backprojection Reconstruction

In this work the Feldkamp, Davis and Kress (FDK) approximation [12] for cone beams was used in the FBP pCT reconstructions. In the FDK approximation, protons must be assigned to a pseudo source position and equispaced lateral and vertical displacement bins. Due to MCS within the imaged object, proton path integrals do not coincide with a uniform sinogram grid. To account for this, each individual proton was rebinned. This rebinning of individual proton histories was calculated with the information provided by the silicon tracking modules and a straight line path assumption through the reconstruction space.

In our work, protons were assigned to 2 degree angular bins, 1 mm lateral displacement bins and 5 mm vertical bins. The Ram-Lak [13] filter was used to avoid further degradations in spatial resolution.

C. Proton CT Iterative Projection Reconstruction

The primary advantage of using iterative projection algorithms is the ability to incorporate a more realistic proton path model in the reconstruction. In this work, the most likely path formalism of Schulte *et al.* [7] was used to improve spatial resolution.

The calculation of proton paths with the MLP subroutine is computationally expensive. This has led to the adoption of parallelizable block-iterative or string-averaging projection algorithms executed on multi-core processors to allow for fast reconstructions. The block-iterative diagonally relaxed orthogonal projections (DROP) [9] scheme was used in the current work, as promising results had been found in our previous work [14]. A recently developed method that takes variations in the voxel-intersection length into account [15] was used for the calculation of system matrix elements.

Most studies with iterative algorithms begin the cyclic reconstruction process with a uniform initial image estimate. In the current work, we reconstructed images with both a uniform initial image estimate corresponding to the relative stopping power of air, and with the FBP-reconstructed image as the initial estimate. 10 cycles were carried out for each reconstruction approach, where a cycle refers to one complete sweep of all collected proton histories with the DROP algorithm.

D. Image Quality Measures

Although 3D images were reconstructed with each approach, only the central slice was used in the analysis of image quality.

1. Quantitative accuracy

The primary motivation for developing our pCT system is the need to directly reconstruct relative proton stopping powers for use in proton therapy treatment planning. In this application, quantitative accuracy of the reconstructed images is important. Histogram analysis is a useful method for assessing quantitative accuracy of the reconstructed images. We also used the relative error (ϵ_n) to obtain a single value to describe the quantitative accuracy. This was calculated as

$$\epsilon_n = \frac{\sum_j |x'_j - x^n_j|}{\sum_j |x'_j|}. \quad (1)$$

Here, x'_j is the relative stopping power in voxel j of the phantom and x^n_j is the reconstructed relative stopping power in voxel j after n cycles.

2. Spatial resolution

Spatial resolution of the reconstructed images was quantified with the 2D modulation transfer function (MTF). For this measure, the point spread function (PSF) of the central dense rectangular prism in Fig. 1(a) was used. Following reconstruction, a 2D FFT of a 32×32 pixel region of interest centered on the PSF was carried out. The MTF was obtained by averaging the magnitude of the first row and

column of the resulting spatial frequency representation of the image.

3. Density resolution

Density resolution was assessed with the contrast discrimination function (CDF). This is an objective statistical analysis method for determining the minimum contrast required to discriminate an object of a certain size from the surrounding tissue. The CDF is calculated by dividing the reconstructed image of a uniform phantom into a grid, where the sizes of the grid elements correspond to the size of the “object” to be discriminated. The distribution of mean pixel values within the grid elements can be used to determine the minimum contrast detectable with a given confidence level. See [16] for a complete description of the method. The uniform phantom (Fig. 1(b)) data set was used for this measure. In the analysis, “objects” ranging from 1×1 to 10×10 pixels in size were considered.

III. RESULTS

The reconstructed images from the density resolution phantom and spatial resolution phantom pCT data sets are shown in Fig. 2. The images reconstructed with DROP correspond to the cycle of minimum relative error. This was cycle 9 for the uniform initial image estimate and cycle 3 for the FBP initial image estimate. Thus, the combined reconstruction algorithm reached the minimum relative error after fewer iterations.

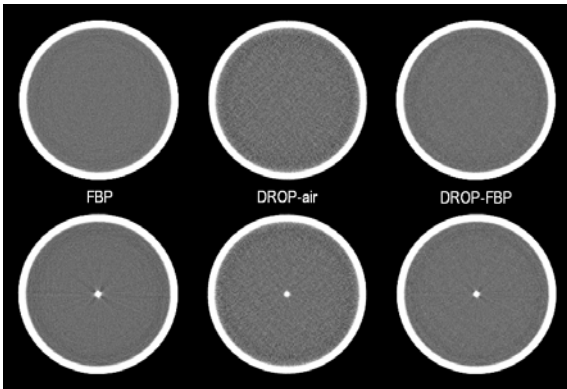


Fig. 2. Uniform and point source images reconstructed with FBP (left), DROP with a uniform initial image estimate (center) and DROP with an FBP-reconstructed initial image estimate (right).

A. Quantitative Accuracy

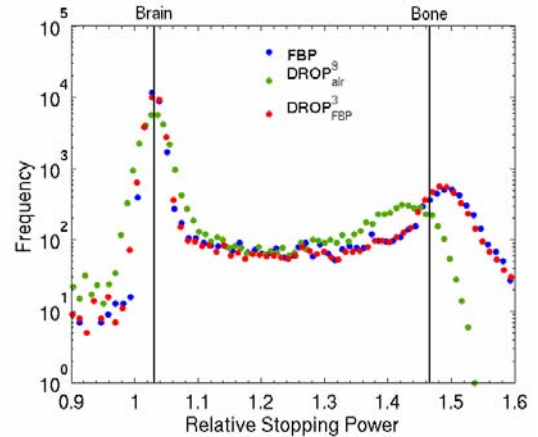


Fig. 3. Histograms of the reconstructed images. The vertical lines correspond to the relative stopping power of the true phantom materials. The numbers in superscript for the DROP reconstructions refer to the cycle of minimum relative error.

Histograms of the reconstructed images from Fig. 2 are shown in Fig. 3. All reconstruction approaches were found to match the phantom brain stopping power value within peak fitting uncertainty. The image reconstructed with FBP was found to overestimate the relative stopping power of bone regions by 2.1%. When DROP was used with a uniform initial image estimate assuming the relative stopping power of air, bone stopping powers were initially underestimated and iteratively improved through the reconstruction process. After 9 cycles, the peak value of the bone region was underestimated by 2.1%. The image reconstructed with DROP and an FBP-reconstructed initial image estimate iteratively reduced the overestimation of the bone relative stopping power resulting from FBP. By the end of the 3rd cycle, the overestimation had been reduced to 1.6%.

B. Spatial Resolution

It was found that the spatial resolution resulting from an FBP reconstruction was 0.089 lp/pixel for an MTF value of 0.5. This was inferior to both images reconstructed with DROP, for which 0.116 lp/pixel and 0.111 lp/pixel at an MTF value of 0.5 were found for the uniform and FBP-reconstructed initial image estimates, respectively. Fig. 4 demonstrates the improvement in spatial resolution with an increasing number of cycles for the iterative procedure.

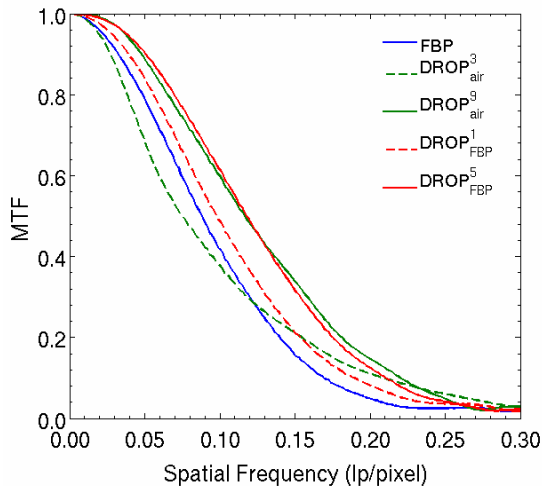


Fig. 4. Modulation transfer function for images reconstructed with FBP, DROP with a uniform initial image estimate and DROP with an FBP-reconstructed initial image estimate. The dashed lines represent the MTF at an early cycle of the iterative procedure and the solid lines represent the MTF at a later cycle. Cycle number is shown in superscript. Spatial resolution increases with increasing cycle number.

C. Density Resolution

The image reconstructed with FBP was found to require less contrast than either DROP reconstructions to discriminate an object of a given size from background. That is, superior density resolution was observed for FBP. It was found that an object of 2.4×2.4 mm and 1% contrast could be discriminated with 95% confidence level when reconstructing with FBP. This is compared with objects 4.4×4.4 and 2.8×2.8 mm in size for the images reconstructed with DROP starting from air and FBP, respectively. The decrease in density resolution with increasing number of cycles is shown in Fig. 5.

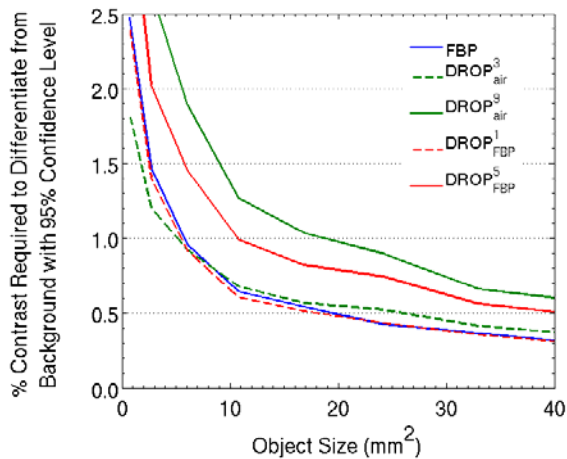


Fig. 5. Contrast discrimination function for the various reconstruction approaches. Dashed lines represent an early cycle of the iterative procedure while solid lines represent later cycles of the iterative procedure. The cycle number is shown in superscript.

IV. DISCUSSION

There are a number of factors to consider when selecting the image reconstruction algorithm to use for pCT. If the images are to be used for proton therapy treatment planning,

quantitative accuracy and the ability to delineate organ boundaries are both important aspects. If the images are to be used in pre-treatment patient positioning, spatial resolution and reconstruction time are key.

From the results of the current work, it was demonstrated that iterative projection algorithms are better suited to pCT treatment planning applications than the FBP algorithm. While FBP-reconstructed images display good density resolution, the straight line path assumption leads to an underestimation of the proton path length, which, in turn, results in an overestimation of the stopping power in the reconstructed images. This effect is more evident in higher Z materials where the degree of MCS is larger (see Fig. 3). When MCS is accounted for by an iterative projection algorithm that incorporates the MLP formalism, this effect is significantly reduced. On the other hand, fast FBP algorithms may be used in pCT based image-guided alignment verification where high reconstruction speed is a requirement, but exact reproduction of stopping power is not crucial.

The ability to delineate organ boundaries depends on both spatial and density resolution. It was found that superior spatial resolution could be achieved with an iterative projection algorithm starting from a uniform initial image in comparison to an FBP reconstruction, due to the MLP subroutine. In contrast, superior density resolution was found in images reconstructed with FBP than those reconstructed with an iterative projection algorithm starting from a uniform initial estimate. Images reconstructed with an iterative projection algorithm starting from an FBP-reconstructed estimate were found to produce better spatial resolution than that achieved with FBP alone and better density resolution than that found with DROP starting from a uniform initial image estimate.

An ideal pCT reconstruction algorithm would have the flexibility to incorporate the MLP formalism into the reconstruction procedure and also be robust in dealing with noisy projection data. With this premise, we are currently investigating the use of perturbation resilient total variation superiorization [17] in pCT reconstruction.

V. CONCLUSIONS

Proton CT is a novel imaging modality that has potential applications in the field of proton radiation therapy planning and image guidance. Previous studies with pCT have made use of either FBP or iterative projection methods with a uniform initial image estimate for image reconstruction. While FBP-reconstructed images were found to display desirable density resolution, images lacked spatial resolution, and vice versa for the iterative algorithms. In this work it was demonstrated that if FBP is used as the initial image estimate for an iterative projection algorithm, images can be reconstructed with better spatial resolution than that achieved with FBP alone and better density resolution than DROP starting from a uniform initial image estimate. It was also found that the use of a most likely proton path model that

accounts for MCS leads to more accurate reconstruction of stopping powers of high Z materials, such as bone, which is important for treatment planning applications.

REFERENCES

- [1] A.M. Cormack and A.M. Koehler, "Quantitative proton tomography: Preliminary experiments", *Phys. Med. Biol.*, vol. 21, pp. 560–569, 1976.
- [2] K.M. Hanson, J.N. Bradbury, T.M. Cannon, R.L. Hutson, D.B. Laubacher, R.J. Macek, M.A. Paciotti and C.A. Taylor, "Computed tomography using proton energy loss", *Phys. Med. Biol.*, vol. 26, pp. 965–983, 1981.
- [3] R. Schulte, V. Bashkurov, T. Li, Z. Liang, K. Mueller, J. Heimann, L.R. Johnson, B. Keeney, H.F.-W. Sadrozinski, A. Seiden, D.C. Williams, L. Zhang, Z. Li, S. Peggs, T. Satogata, and C. Woody, "Conceptual design of a proton computed tomography system for applications in proton radiation therapy", *IEEE Trans. Nuc. Sci.*, vol. 51, pp. 866–872, 2004.
- [4] R.W. Schulte, V. Bashkurov, M.C. Loss Klock, T. Li, A.J. Wroe, I. Evseev, D.C. Williams, T. Satogata, "Density resolution of proton computed tomography", *Med. Phys.*, vol. 32, pp. 1035–1046, 2005.
- [5] T. Li, Z. Liang, J.V. Singanallur, T.J. Satogata, D.C. Williams and R.W. Schulte, "Reconstruction for proton computed tomography by tracing proton trajectories: A Monte Carlo study", *Med. Phys.*, vol. 33, pp. 699–706, 2006.
- [6] D.C. Williams, "The most likely path of an energetic charged particle through a uniform medium", *Phys. Med. Biol.*, vol. 49, pp. 2899–2911, 2004.
- [7] R.W. Schulte, S.N. Penfold, J.T. Tafas and K.E. Schubert, "A maximum likelihood proton path formalism for application in proton computed tomography", *Med. Phys.*, vol. 35, pp. 4849–4856, 2008.
- [8] R. Gordon, R. Bender and G.T. Herman, "Algebraic reconstruction techniques (ART) for three-dimensional electron microscopy and x-ray photography," *Jour. Theor. Biol.*, vol. 29, pp. 471–481, 1970.
- [9] Y. Censor, T. Elfving, G.T. Herman, and T. Nikazad, "On diagonally-relaxed orthogonal projection methods", *SIAM Jour. Sci. Comp.*, vol. 30, pp. 473–504, 2008.
- [10] S. Agostinelli, J. Allison, K. Amako, J. Apostolakis et al., "GEANT4—A simulation toolkit," *Nucl. Instrum. Meth. Phys. Res. A*, vol. 506, pp. 250–303, 2003.
- [11] ICRP 1975 Report of the Task Group on Reference Man *ICRP Publication 23*.
- [12] L.A. Feldkamp, L.C. Davis, and J.W. Kress, "Practical cone-beam algorithm", *J. Opt. Soc. Amer. A*, vol. 6, pp. 612–619, 1984.
- [13] G.N. Ramachandran and A.V. Lakshminarayanan, "Three-dimensional reconstruction from radiographs and electron micrographs: Application of convolutions instead of Fourier transforms", *Proc. Nat. Acad. Sci. USA*, vol. 68, pp. 2236–2240, 1971.
- [14] S.N. Penfold, R.W. Schulte, Y. Censor, V. Bashkurov, S. McAllister, K.E. Schubert, and A.B. Rosenfeld, "Block-iterative and string-averaging projection algorithms in proton computed tomography image reconstruction", In: *Biomedical Mathematics: Promising Directions in Imaging, Therapy Planning and Inverse Problems*, Y. Censor, M. Jiang and G. Wang (Eds), Medical Physics Publishing, Madison, WI, to be published.
- [15] S.N. Penfold, R.W. Schulte, K.E. Schubert, and A.B. Rosenfeld, "A more accurate reconstruction system matrix for quantitative proton computed tomography", *Med. Phys.*, vol. 36, pp. 4511–4518, 2009.
- [16] E.H. Chao, T.L. Toth, N.B. Bromberg, E.C. Williams, S.H. Fox, and D.A. Carleton, "A statistical method of defining low contrast detectability", *Radiology*, vol. 217, p162, 2000.
- [17] D. Butnariu, R. Davidi, G.T. Herman, and I.G. Kazantsev, "Stable convergence behavior under summable perturbations of a class of projection methods for convex feasibility and optimization problems", *IEEE J. Sel. Top. Sig. Proc.*, vol. 1, pp. 540–547, 2007.